USE OF SIZE FREQUENCY DISTRIBUTIONS IN THE INTERPRETATION OF PLANETARY SURFACE MATERIALS. L.C. Kah[1], M. Minitti[2], E. Cardarelli[3], N. Mangold[4], Y. Liu[3], S. Gupta[5], J. Hurowitz[6], J.I. Núñez[7], R.C. Wiens[8], A. Yingst[9]; [1]Earth & Planetary Sciences, University of Tennessee, Knoxville TN, 37996, lckah@utk.edu; [2]Framework, [3]JPL/Caltech, [4]Univ Nantes, [5]Imperial College London, [6]Stonybrook Univ, [7]JHU/APL, [8]LANL, [9]PSI.

Introduction: Size frequency distributions have a broad utility that derives from their distinctive shapes, which provide information about the growth of crystals (e.g., nucleation and growth of crystals in an open system), changes in crystal size during maturation (e.g., Ostwald ripening, wherein larger crystals grow at the expense of smaller crystals), and the physical segregation of size populations (e.g., physical sorting and transport). Such distributions may also provide a mechanism of deciphering igneous from sedimentary emplacement where the chemistry is ambiguous.

The exploration of size frequency distributions in both igneous and sedimentary materials goes back nearly a century, yet the greatest advances in our understanding have occurred in the last 50 years. These advances result from a combination of the theoretical exploration of the chemistry and physics involved in size frequency distributions [1,2], the measurement of natural samples, and enhanced interpretation via experimental reconstruction of size frequency distributions [3,4]. More recently, efforts have been used to extend understanding through computerized models that aid in the measurement, and in the critical comparison of 2D and 3D datasets [5,6].

Despite these advances, there has been surprisingly little overlap between the igneous, engineering, and sedimentary subdisciplines. In the planetary sciences, for instance, there is a rich literature base that focuses Crystal Size Distributions (CSDs) of meteorites to explore their igneous emplacement and potential geographic origin [7,8]. Similarly, the size frequency distributions of sedimentary materials on Mars that have been used in the pre-landing assessment and prediction of potential hazards [9], and to explore details of wind regime responsible for the generation of aeolian bedforms [10,11]. Size frequency distributions have even been used to explore potential fluid saturation states represented by chemical precipitates such as martian 'blueberries' [12], and have even been used, albeit not entirely successfully, to argue for the potential of magnetite phases in the martian meteorite ALH 84001 to be biogenic in origin [13].

Here we review the basic understanding of size frequency distributions and the differences in shape that develop in response to geologic processes associated with the nucleation and growth of primary crystals, maturation (or ripening) of crystals, and the physical transport of disaggregated materials. In this initial comparison of features between subdisciplines, we will focus on the differences in the shape of 2D distributions extracted from visual images and explore the extent to which such comparison may permit the first-order differentiation between (or constraint on) igneous or sedimentary emplacement of surface materials that are imaged by landers and rovers.

Crystal Size Distributions: CSDs in crystalline materials fundamentally derive from patterns of crystal nucleation and growth, and therefore allow quantitative measure of the kinetics of crystallization based on textural observations. In magmatic systems, cooling results in the nucleation of a crystalline phase, and crystal growth continues until magma quenching or until the magma no longer supports growth of the mineral phase. Magmatic crystallization, as observed in CSDs is best described by an asymptotic distribution, which reflects continuous nucleation in and growth in an open system. Plotted on a semi-log plot, such a distribution forms a line of negative slope. Modification of this archetypical CSD can result from, (1) annealing of grains, which results in a downturn of the CSD at the finest grain sizes, (2) grain settling, which results in a flattening of the CSD at larger grain sizes, or (3) magma mixing, which results in kinking of the CSD.

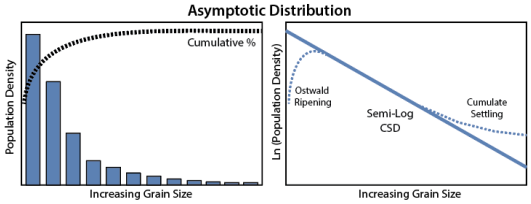

Fig. 1. An asymptotic distribution is representative of most igneous systems, noting common modifications.

Ambiguity arises in CSDs in the downturn at small crystal sizes. Such downturn is consistent with grain modification via Ostwald ripening but is also consistent with a simple model for nucleation in which pre-nucleation clusters reach a certain size threshold before crystal nucleation, which results in a decay-rate, or lognormal, nucleation profile.

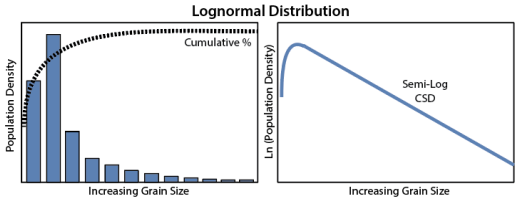

Fig. 2. A lognormal distribution mimics CSDs common to magmatic processes and is the most common CSD pattern observed in the precipitation of chemical sediments.

Experiments on chemical precipitates permit the exploration of grain modification under closed system conditions. Here, Ostwald ripening (which is typically limited in igneous systems by cooling and quenching of the magmatic system) continues to modify the system through the dissolution of the finest grain sizes and growth of coarser materials. Through time, the mode of the CSD migrates to the right until it ultimately reaches steady state conditions.

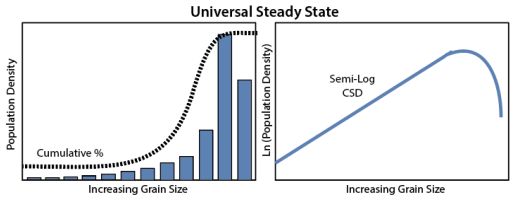

Fig. 3. Universal steady state CSD which represents the steady state endmember of Ostwald ripening.

Grain Size Distributions: By contrast to CSDs, sedimentary grain size distributions reflect not only the original formational processes of grains, but the processes of disaggregation of a protolith, dynamic transport, and the ultimate deposition of grains. In this case, the size distribution of deposited sediment is a function of (1) grains available for transport (i.e., what is there), (2) the density difference between fluid and sediment (i.e., what can be picked up), (3) fluid velocity profile resulting in grain entrainment (i.e., what is picked up), (4) the rate of fluid deceleration and grain deposition (i.e., what can no longer be carried).

The differences in density between grains and the most common fluids (i.e., water or air) typically results in a narrow distribution in particle size, and changes in fluid velocity during deposition result in skewing of the profile to finer or coarser grains.

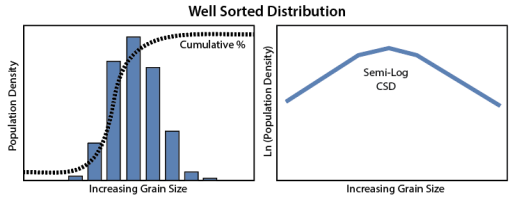

Figure 4. The typical size distribution of a well-sorted sedimentary deposit records a very different CSD shape.

An Example from Jezero Crater: Size frequency distributions have been constructed for twelve unique targets within the Séítah region of Jezero crater. Séítah rocks are the oldest materials exposed within Jezero crater and are interpreted as an ultramafic, olivine cumulate deposit [see 2022 LPSC abstracts]. 2D grain sizes show a tight grain size distribution, with a broadly normal distribution. Grain size data show little variation between geographic regions save the uppermost Séítah targets, which show a similar distribution at finer sizes.

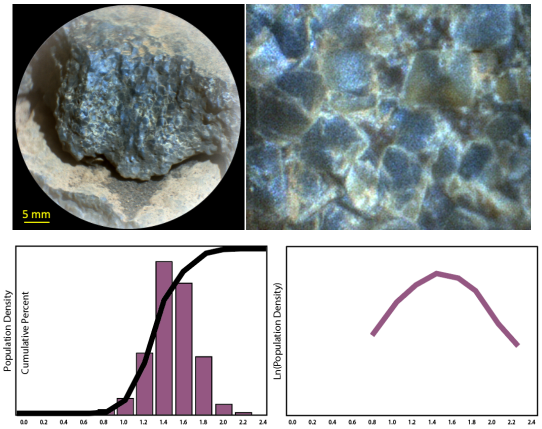

Fig. 5. SuperCam RMI of target Cine, showing euhedral to subhedral crystalline olivine. Most Séítah samples (purple) contain sand-sized grains with a mean of 1.53±0.08 mm.

Implications: At first glance, Séítah materials show size frequency distributions characteristic of dynamic sorting that is more typical of sedimentary materials. A sedimentary interpretation requires explanation of the apparent mineralogical sorting and strong prevalence of euhedral monocrystalline olivine. Similar distributions, however, are not common in magmatic rocks, where even cumulate deposits tend to have a strongly asymptotic primary CSD [14,15]. Distributions with a strong downturn in the finer grain sizes can theoretically form, however, from dynamic cumulate settling within a magma that also experiences extensive Ostwald ripening [3]. Because Séítah materials appear be uncompacted cumulates, with up to 45% intercumulus, any hypothesis for cumulate formation needs to account for a high degree of grain ripening suggested by the CSDs, potentially by changes in the thermal behavior of the pre-eruptive magma [16]. Alternatively, apparent absence of olivine within the finer crystal sizes may result from image resolution or the potential for alteration to affect finer crystals within the deposit resulting in the loss of fine olivine and the addition of alteration minerals within the intercumulus regions.

References: [1] Marsh B. D. (1988) *CMP,* 277-291. [2] Eberl D. D. et al. (1998) Am J Sci, 499-533. [3] Cashman K. and Marsh B. (1988). *CMP*, 292-305 [4] Kile D. E. et al. (2000) *GCA*, 2937-2950. [5] Jerram D. A. et al. (2010) *Geosphere*, 537-548. [6] Mock A. and Jerram D. (2005). J Petrol, 1525–1541. [7] Udry A. and Day J. M. D. (2018) *GCA*, 292-315.[8] Filiberto J. et al. (2018) *JGR Planets*, 1823-1841. [9] Golombek M. P. et al. (2003) *JGR*, 8086. [10] Jerolmack D. J. et al. (2006) *JGR Planets*, E12SO2.[11] Weitz C. M. et al. (2018) *GRL*, 9471-9479.[12] Eberl D. D. (2022) *Am Mineral*, 153-155. [13] Jandaka P. (2013) *Am Mineral*, 2105-2114.[14] Jerram D. A. et al. (2003) *J Petrol*, 2033-2051. [15] Mao Y-J. et al. (2018) *J Petrol*, 1701-1730. [16] Simakin A. G. and Bindeman I. N. (2008) *J Volc Geotherm Res*, 997-1010.